ACS Medicinal Chemistry Letters

Featured Letter

pubs.acs.org/acsmedchemlett

Discovery of AZD2716: A Novel Secreted Phospholipase A_2 ($sPLA_2$) Inhibitor for the Treatment of Coronary Artery Disease

Fabrizio Giordanetto,*[,†,▽] Daniel Pettersen,*[,†] Ingemar Starke,[†] Peter Nordberg,[†] Mikael Dahlström,[†] Laurent Knerr,[†] Nidhal Selmi,[†] Birgitta Rosengren,[‡] Lars-Olof Larsson,[§] Jenny Sandmark,[∥] Marie Castaldo,[⊥] Niek Dekker,[⊥] Ulla Karlsson,[#] and Eva Hurt-Camejo[‡]

[†]Cardiovascular and Metabolic Diseases, Innovative Medicines and Early Development Biotech Unit Departments of Medicinal Chemistry, [‡]Bioscience, [§]DMPK, [∥]Discovery Sciences Departments of Structure & Biophysics, [⊥]Reagents and Assay Development, and [#]Screening Sciences and Sample Management, Astrazeneca, Mölndal, Pepparedsleden 1, SE-431 83 Mölndal, Sweden

Supporting Information

ABSTRACT: Expedited structure-based optimization of the initial fragment hit **1** led to the design of (*R*)-7 (AZD2716) a novel, potent secreted phospholipase A_2 ($sPLA_2$) inhibitor with excellent preclinical pharmacokinetic properties across species, clear *in vivo* efficacy, and minimized safety risk. Based on accumulated profiling data, (*R*)-7 was selected as a clinical candidate for the treatment of coronary artery disease.

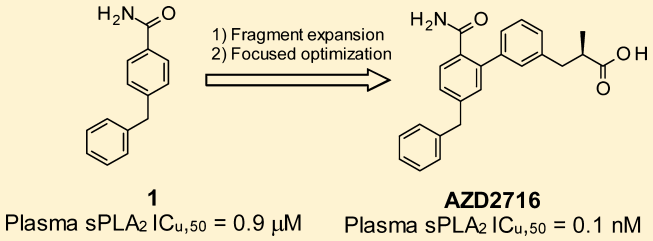

KEYWORDS: *Secreted phospholipase A_2, $sPLA_2$, inhibitor, fragment-based drug discovery, fragment screening, atherosclerosis, coronary artery disease*

Secreted phospholipase A_2 ($sPLA_2$) are enzymes that hydrolyze the acyl ester at the sn-2 position of sn-3 glycerophospholipids,[1] a process characterized by complex interfacial kinetics of substrate−enzyme binding and catalysis.[2] Eleven $sPLA_2$ enzymes (group Ib-XIIb) have so far been identified in mammals,[3−5] several of which have been detected in human atherosclerotic lesions.[6] Among these, group IIa, V, and X $sPLA_2$ isoforms are present in human carotid atherosclerotic lesions and have been associated with disease progression. They have been implicated in several proatherogenic actions in the arterial wall.[7−9] Due to their hydrolytic action on lipoprotein phospholipids, $sPLA_2$s promote lipid accumulation, induce significant lipoprotein remodeling, macrophage activation, and foam cell formation.[10,11] Furthermore, as the rate-limiting step in eicosanoid production, $sPLA_2$-mediated release of arachidonic acid from the *sn*-2 position of phospholipids renders them highly pro-inflammatory enzymes.[10,11] In addition, epidemiological data has shown that increased levels of $sPLA_2$ protein and $sPLA_2$ activity are independently associated with risk of cardiovascular events and prevalence of atherosclerosis.[11] Owing to the pivotal role of $sPLA_2$s in regulating lipoprotein function and inflammatory mechanisms, two crucial components of atherogenesis, $sPLA_2$ inhibitors[12] could be useful for the treatment of atherosclerosis. Interestingly, the archetypal $sPLA_2$ inhibitor varespladib methyl (Figure 1) was evaluated in short duration clinical trials for the treatment of rheumatoid arthritis and acute coronary syndrome with negative results.[13,14]

We thus set out to identify novel $sPLA_2$ inhibitors that could be used in longer term coronary artery disease-based clinical studies to more properly assess the relevance of their lipoprotein-modifying effects[15−17] on cardiovascular disease, alongside their anti-inflammatory properties.

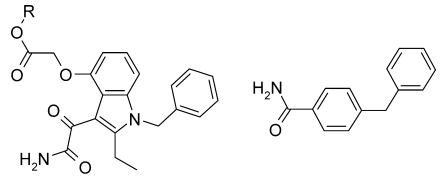

Figure 1. $sPLA_2$ inhibitor varespladib methyl, its active metabolite varespladib, and initial fragment hit **1**.

Given the competitive landscape, medicinal chemistry precedents and available structural information for $sPLA_2$ enzymes, we opted for a structure-based fragment approach to maximize the chances of novelty and developability.[18] Analysis of potency data in combination with the available ligand-bound $sPLA_2$ crystal structures[19] indicated that primary amides are extremely effective $sPLA_2$ warheads, as they establish three hydrogen bonds with $sPLA_2$ and one coordination bond with the catalytic calcium ion. We assembled a selection of primary aromatic carboxamide-containing fragments (heavy atom count ≥10 and ≤18) by mining in house biochemical and biophysical assay data against the $sPLA_2$-IIa and $sPLA_2$-X isoforms. The selection was based on activity against $sPLA_2$-IIa,

Received: May 3, 2016
Accepted: August 9, 2016
Published: August 9, 2016

DOI: 10.1021/acsmedchemlett.6b00188
ACS Med. Chem. Lett. 2016, 7, 884−889

which is the most widely expressed isoform in humans,[20] but also on inspection of crystal structures and chemical evolution potential.

The triaging process identified compound **1** (LE: 0.39) originating from a legacy fragment/HTS campaign as the most promising fragment lead. As the translatability to a clinical setting was of special importance, we also triaged the activities for $sPLA_2$ activity inhibition in human plasma (the mode-of-action biomarker to be used in clinical trials), as measured using a previously established protocol.[21]

Compound **1** inhibited $sPLA_2$-IIa (IC_{50}: 24 μM) and human plasma $sPLA_2$ activity ($IC_{u,50}$: 0.9 μM) in a concentration dependent manner (Table 1). Going forward, as plasma $sPLA_2$ activity is the result of various $sPLA_2$ isoforms and we were interested in identifying a broad spectrum $sPLA_2$ inhibitor, we also monitored inhibition of $sPLA_2$-V and $sPLA_2$-X, given their potential role in lipoprotein modulation.[16] Lastly, to avoid the need for a prodrug strategy (e.g., varespladib methyl) we carefully evaluated compound lipophilicity against passive permeability, solubility, and metabolic stability, prior to verifying the pharmacokinetic (PK) and pharmacodynamic (PD) profile *in vivo*.

Table 1. Initial Profile for the Fragment Hit 1

entry	$sPLA_2$-IIa IC_{50} (μM)	plasma $IC_{u,50}$ (μM)[a]	F_u (%)	LE/LLE[b]
varespladib	0.028	0.008	12.5	0.37/7.2
1	24	0.9	1.8	0.39/2.2

[a]Calculated as plasma $sPLA_2$ IC_{50} (μM) × compound's unbound fraction in human plasma (F_u)/100. F_u = 100 − human protein binding (%). [b]Ligand efficiency, LE (kcal/mol/HAC), calculated as $-RT$ ln($sPLA_2$-IIa IC_{50})/heavy atom count. Ligand lipophilicity efficiency (LLE) calculated as pIC_{50} ($sPLA_2$-IIa) − logD.

The crystal structure of **1** bound to $sPLA_2$-X confirmed the binding mode of the primary amide, with hydrogen-bonding to $sPLA_2$-X's G28, H46, and D47 (corresponding to sPLA2-IIa G29, H47, and D48) and coordination to the calcium ion was observed, as shown in Figure 2. Additionally, the 4-benzyl substituent was located in a lipophilic pocket consisting of residues I2, L5, A6, V9, P17, I18, and M21 (corresponding to L2, F5, H6, I9, A17, A18, and G22 in $sPLA_2$-IIa, Figure 2). While the two $sPLA_2$ isoforms are identical in the amide coordinating residues, the lipophilic pocket that accommodates the benzyl group is slightly smaller in sPLA2-IIa. However, superposition of the $sPLA_2$-IIa and $sPLA_2$-X crystal structures suggested that the benzyl group of **1** could fit in the slightly smaller $sPLA_2$-IIa pocket.

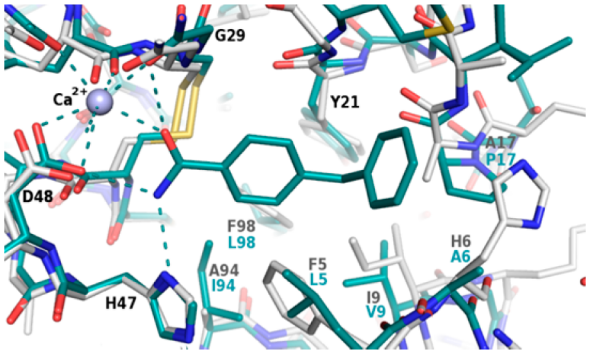

Figure 2. Superposition of the crystal structure of **1** bound to $sPLA_2$-X (cyan) and a crystal structure of $sPLA_2$-IIa (gray). Residues that differ between the two isoforms are labeled in cyan and gray, respectively. The calcium ion is depicted as a purple sphere and hydrogen bonds are displayed as dashed lines.

We therefore devised a chemical exploration strategy starting from the binding mode of **1**. Here, special effort was placed upon establishing a second coordination bond to the catalytic calcium ion. The reasoning was 2-fold: (a) to increase affinity and functional inhibition of the enzyme as a result of a bidentate calcium chelate and additional van der Waals contact with the enzyme, and (b) to allow a more balanced lipophilicity profile of the final compounds as the additional calcium interacting moiety was anticipated to be a carboxylic acid. The *ortho* position of the benzamide ring was identified as a favorable substitution vector to deploy such a strategy. Based on iterative molecular modeling and careful consideration of theoretical affinity gain and ligand efficiency prediction, we synthesized compounds **2**−**6**, according to Scheme 1 (for compound **4** refer to Scheme 2). Key steps involved the formation of the boronic acid by *ortho* lithiation[22] of the 4-benzylbenzonitrile (step b) followed by a Suzuki−Miyaura coupling and a controlled hydrolysis (step d) to generate both the amide and carboxylic acid functions (Scheme 1).

Scheme 1. General Synthesis of Compounds 2, 3, 5, and 6[a]

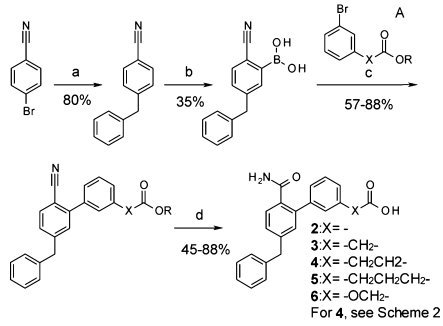

[a]Conditions: (a) benzylzinc bromide, $Pd(Ph_3)_4$, THF, 60 °C. (b) 1. *n*BuLi, tetramethylpiperidine; 2. $B(OiPr)_3$, THF −78 °C. (c) Compound **2**, **3**, **5**: 3-bromophenyl carboxylic acid **A**, $PdCl_2$(dppf), Cs_2CO_3, DMF, 60−90 °C. Compound **6**: $Pd(P(Ph_3)_4$, Cs2CO3, DMF 90. (d) Compound **2**, **3**, **5**: *n*-propanol/H_2O (10:1), KOH (10 equiv), 80−100 °C, or THF, H_2SO_4. Compound **6**: KOH (10 equiv), MeOH/H_2O, microwave 130 °C, 20 min.

Introduction of a 3-benzoic acid moiety at the 2-position of 4-benzylbenzamide **1**, albeit nonoptimal, confirmed the potential for growth at that position (**2**, Table 2). Progressive elongation at the carboxylic acid position by introduction of methylene units (**3**−**5**) had a parabolic effect on potency, with the 3-phenylpropionic acid side chain yielding the most potent and ligand efficient derivative (**4**, Table 2). Replacement of the benzylic methylene by an ether oxygen or further elongating the hydrocarbon chain were not tolerated (cf. **5** and **6**, Table 2), hinting at a specific conformational requirement for the carboxylic acid-containing side chain. The cocrystal structure of $sPLA_2$-IIa and **4** confirmed the previously hypothesized ligand-mediated calcium chelation, as displayed in Figure 3.

The carbonyl oxygen atom of the amide group of **4** provided the first coordination bond to calcium, analogously to **1**. The carboxylate moiety established the second coordination bond to calcium (d = 2.4 Å) and a hydrogen bond to the backbone

DOI: 10.1021/acsmedchemlett.6b00188
ACS Med. Chem. Lett. 2016, 7, 884−889

Scheme 2. General Synthesis of sPLA$_2$ Inhibitors 4 and 7−9[a]

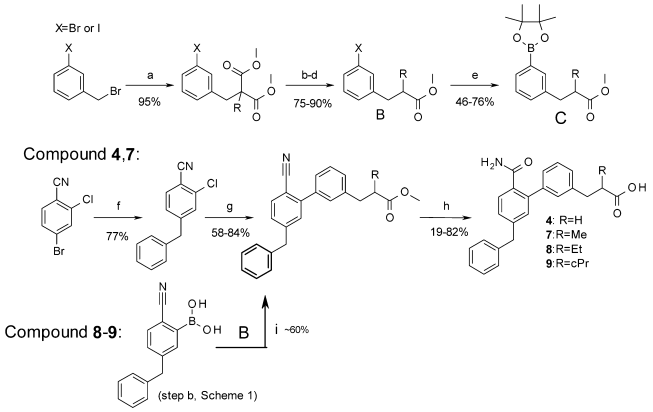

[a]Conditions: (a) appropriate malonate, Cs_2CO_3, DMF, 70 °C, 2 h. (b) NaOH (4 equiv), H_2O/MeOH 3:1 80 °C 2 h. (c) HOAc (3 M), reflux. (d) HCl, MeOH 60 °C, 2.5 h. (e) $(Bpin)_2$ (1.3 equiv), KOAc (2.5 equiv), $PdCl_2$(dppf) (6.5 mol %), dioxane, 90 °C. (f) BnZnBr (1.5 equiv, 0.5 M in THF), $Pd(PPh_3)_4$ (5 mol %), THF, 60 °C, 2 h. (g) Compound **4**: 3-(3-methoxy-3-oxopropyl)phenylboronic acid (commercial), $Pd(Ph_3)_4$. Compound **7**: $PdCl_2$(dbpf) (5 mol %), C. Cs_2CO_3, DMF, 90 °C, 1.5 h. (h) *n*-Propanol/H_2O (10:1), KOH (10 equiv), 80−100 °C. (i) **B**, $PdCl_2$(dppf), Cs_2CO_3, DMF, 90 °C.

amide group of G31, as shown in Figure 3, while the additional phenyl ring made significant van der Waals contacts with the side chains of L2, G29, and V30. The 4-benzylbenzamide component of **4** displayed a similar interaction pattern as in **1**, except for the benzamide ring, which was rotated by ca. 50 degrees. This rotation is induced by the introduction of the substituent at the 2-position, and in the case of sPLA$_2$-X, this comes with a penalty. This is exemplified by **2** and **3**, where the affinity gain is very limited, despite the addition of more lipophilic interactions (Table 2). In type IIa, however, this conformational lock is further stabilized by an edge-to-face π interaction with F5, which is not available in sPLA2-X. This is reflected by the steep improvement in affinity when adding the substituents. For example, **3** despite having a linker too short to form the additional calcium interaction still gains more than 300-fold in affinity. This is further improved by the propanoic acid side chain of **4** where the second calcium coordination bond is properly established leading to a 2000-fold increase in

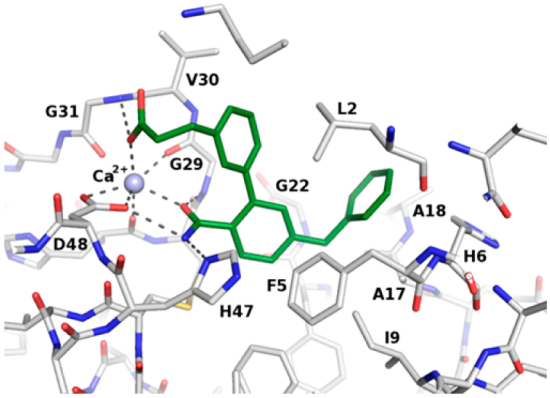

Figure 3. Cocrystal structure of **4** bound to sPLA$_2$-IIa. The calcium ion is depicted as a purple sphere, and relevant hydrogen bonds are displayed as dashed lines.

Table 2. sPLA$_2$ Potency and Ligand Efficiencies for Compounds 2−6[a]

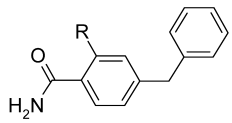

Entry	R	sPLA$_2$-IIa IC_{50} (μM)	sPLA$_2$-V IC_{50} (μM)	sPLA$_2$-X IC_{50} (μM)	Plasma $IC_{u,50}$ (μM)[b]	LE/LLE[c]
varespladib		0.028	0.12	0.041	0.008	0.37/7.2
1		24	NA[d]	2.2	0.9	0.39/2.2
2	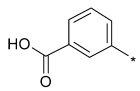	0.91	>10	NA[c]	NA[d]	0.33/4.9
3	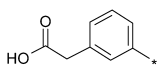	0.07	1.4	1.1	0.04	0.38/5.9
4	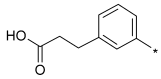	0.012	0.36	0.28	0.007	0.4/6.4
5	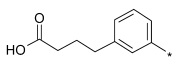	0.11	4.1	5.4	0.03	0.34/5
6	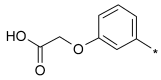	0.19	3.7	3.7	ND[e]	0.34/5.4

[a]Results are mean of at least two experiments. Experimental errors within 20% of value. [b]Calculated as plasma sPLA2 IC_{50} (μM) × compound's unbound fraction in human plasma (F_u)/100. F_u = 100 − human protein binding(%) [c]Ligand efficiency, LE (kcal/mol/HAC), calculated as $-RT$ ln(sPLA$_2$-IIa IC_{50})/heavy atom count. Ligand lipophilicity efficiency (LLE) calculated as pIC_{50} (sPLA$_2$-IIa) − logD. [d]Not active at maximum tested concentration (25 μM). [e]Not determined.

DOI: 10.1021/acsmedchemlett.6b00188
ACS Med. Chem. Lett. 2016, 7, 884−889

potency compared to **1**. The active site of sPLA2-IIa is smaller, F5 (L5 in $sPLA_2$-X) affects the benzamide moiety, and I9 (V9 in $sPLA_2$-X) is located close to the hinge between the two benzyl groups of **1** (d = 3.7 Å), thereby slightly altering the angle in which the 4-benzyl enters the pocket and potentially introducing some strain in the fragment, where the larger pocket of $sPLA_2$-X offers a less restrained binding mode

The high ligand efficiency and potency of **4**, coupled with its marked plasma $sPLA_2$ inhibition ability ($IC_{u,50}$ = 7 nM) triggered a broad characterization campaign to identify potential shortcomings.

As summarized in Table 3, compound **4** proved to be soluble, highly permeable, and metabolically stable; characteristics that translated well *in vivo* with high bioavailability and low systemic clearance recorded in rat and dog (Table 3). This provided a significant improvement over varespladib, which required a methyl ester prodrug approach (i.e., varespladib methyl) to afford moderate oral absorption (F = 40−55%) in the same species. Compound **4** did not show any significant inhibition of cytochrome P450 enzymes or ion channel activity relevant to cardiac function. Nevertheless, **4** inhibited the uptake of pivastatin in HEK293 cells transfected with the human organic anionic transporter polypeptide 1B1 (OATP1B1) at an estimated IC_{50} of 2.2 μM, as shown in Table 3. The OATP1B1 transporter is necessary for statin's hypocholesterolemic action as it mediates their access to the liver compartment where they can then inhibit the function of HMG-CoA reductase.[23−25]

Table 3. Profile[a] of Compound 4

solubility (pH = 7.4) (μM)	98	
P_{app} (10^{-6} cm/s)	40.1	
HEP Cl_{int} (μL/min/10^{-6} cells)	5.2	
hERG, Na_v1.5, IKs, K_v4.3, Ca_v3.2, Ca_v1.2 IC_{50} (μM)	>33.3	
CYP450 IC_{50} (μM)	>20	
OATP1B1 IC_{50} (μM)	2.2	
PK	Rat	Dog
dose i.v./p.o. (μmol/kg)	2/4	1/2
CL (mL/min/kg)	1	0.3
V_{ss} (L/kg)	0.22	0.26
F (%)	81	82

[a]Please see the Supporting Information for experimental details.

Considering that an eventual $sPLA_2$ inhibitor for the treatment of coronary artery disease will need to be coadministered with a statin, as an established standard of care, minimizing the risk for such drug−drug interaction was required. As OATP1B1 recognizes anionic compounds, we reasoned that modification of the molecular environment around the carboxylic acid of **4** might alleviate its interaction with OATP1B1. More specifically, substituting the carbon atom alpha to the carboxylic acid was of special interest as (a) it was postulated to provide a steric impediment to OTAP1B1, (b) it seemed compatible with the binding pocket of the $sPLA_2$-IIa enzyme, and (c) it could enhance potency and/or selectivity through conformational "freezing" of the carboxylic acid side chain via gauche-like effects. Due to structure-based constraints and in order to minimize the impact on compound lipophilicity, we targeted small substituents and synthesized compounds **7**−**9**, following Scheme 2.

According to Scheme 2, the appropriate dimethyl malonate was alkylated using 3-bromobenzyl bromide. The propionic acid derivative was then obtained by hydrolysis, decarboxylation, and re-esterification to yield the methyl ester. Boronylation was accomplished by standard protocols using $(Bpin)_2$ and $PdCl_2$(dppf) to yield the pinacol borane ester, which could be used in the subsequent Suzuki−Miyaura coupling using the benzylated chloro benzonitrile. Finally, racemic **7**−**9** could be obtained by hydrolysis using hydroxide in alcohol/water mixtures (careful monitoring of the reaction to avoid overhydrolysis to the corresponding diacid is needed).

Addition of a methyl group (**7**, Table 4) displayed an isoform-specific effect on potency: while it was neutral at $sPLA_2$-IIa, it enhanced inhibition of $sPLA_2$-V and reduced that of $sPLA_2$-X. Overall, this yielded excellent plasma $sPLA_2$ inhibition ($IC_{u,50}$: 0.1 nM). Remarkably, structural manipulation of the carboxylic acid surroundings by an alpha-methyl group demonstrated the intended effect at a transporter level, and **7** was devoid of OATP1B1 inhibition at the maximum tested concentration (25 μM). Ethyl and cyclopropyl substitutions (**8**, **9**) were not as efficient and had a deleterious effect on metabolic stability in human hepatocytes (cf. **8**, **9**, and **7**, Table 4). We therefore proceeded to separate and characterize the two enantiomers of **7**. In line with expectations, $sPLA_2$ inhibition was affected by stereochemistry, and the R enantiomer proved to be the most active, half-maximally inhibiting $sPLA_2$-IIa, -V, and -X at 10, 40, and 400 nM, respectively (Table 4). As a result, (*R*)-**7** was the most potent

Table 4. $sPLA_2$ Potency and Optimization Parameters for Compounds 4−9

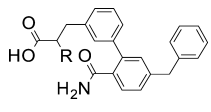

entry	R	$sPLA_2$-IIa IC_{50} (μM)[a]	$sPLA_2$-V IC_{50} (μM)[a]	$sPLA_2$-X IC_{50} (μM)[a]	plasma $IC_{u,50}$ (nM)[b]	HEP Cl_{int} (μL/min/10^{-6} cells)[c]	OATP1B1 IC_{50} (μM)[d]
4	H	0.012	0.36	0.28	7	5.2	2
7	Me	0.011	0.07	0.75	1	9.6	NA[e]
8	Et	0.021	0.07	0.43	0.8	25	ND[f]
9	CyPr	0.018	0.25	0.58	0.9	21	ND[f]
(*S*)-7	(*S*)-Me	0.038	1.2	3.8	ND	9.3	ND[f]
(*R*)-7	(*R*)-Me	0.010	0.04	0.4	0.1	12	NA[e]

[a]Mean of at least two experiments. Experimental errors within 20% of value. [b]Calculated as Plasma $sPLA_2$ IC_{50} (μM) × unbound fraction in human plasma (F_u)/100. [c]Intrinsic clearance of test compounds after incubation with human hepatocytes. [d]Inhibition of pivastatin uptake to HEK293 cells transfected with human OATP1B1. [e]Not active at maximum tested concentration (25 μM). [f]Not determined.

DOI: 10.1021/acsmedchemlett.6b00188
ACS Med. Chem. Lett. 2016, 7, 884−889

plasma $sPLA_2$ inhibitor in this study ($IC_{u,50}$ = 0.1 nM) and, based on its minimized risk for drug−drug interactions with statins, was progressed to further profiling.

When incubated with HepG2 cells, (*R*)-7 effectively inhibited $sPLA_2$ activity (IC_{50} < 14 nM) and suppressed production of $sPLA_2$-IIa (IC_{50} 176 ± 28 nM) via a mechanism not yet elucidated.[7] Importantly, (*R*)-7 demonstrated significant $sPLA_2$ activity inhibition (IC_{50} 56 ± 10 nM) in atherosclerotic plaque homogenates, as obtained from carotid endarterectomy of coronary artery disease patients (N = 7).[26]

In vivo PK analysis of (*R*)-7 showed consistent high bioavailability and low clearance across different animal species, as summarized in Table 5.

Table 5. PK Parameters of Compound (*R*)-7

	mouse	rat	dog	cynomolgus
N i.v./p.o.	2/2	2/2	2/2	2/2
dose i.v./p.o. (μmol/kg)	10/50	2/8	1/3	5/15.8
oral $AUC_{0\text{-}inf}$ (μM × h)	69.7	70	284.1	71.3
Cl (mL/min/kg)	9.2	1	0.2	2.8
V_{ss} (L/kg)	2.8	0.21	0.15	1.1
F (%)	76.3	84	91	81

Building on the observed PK parameters and the *in vitro* $sPLA_2$ inhibition measured in cynomolgus monkey plasma ($IC_{u,50}$ 1 nM), we resolved to evaluate the *in vivo* $sPLA_2$ inhibitory effect of (*R*)-7.

A 30 mg dose of (*R*)-7 was orally administered to cynomolgus monkeys (N = 2), as shown in Figure 4. This generated a concentration-dependent inhibition of $sPLA_2$ activity in plasma ($IC_{u,80}$ = 13 ± 3 nM) that well reflected the time course of (*R*)-7's exposure profile (Figure 4).

In summary, starting from the original fragment hit **1**, two design cycles based on structural information, ligand efficiency reasoning, physicochemical property control, medicinal chemistry tactics, and readily available experimental data resulted in the discovery of (*R*)-7 (AZD2716), a novel, potent $sPLA_2$ inhibitor with excellent PK properties, *in vivo* efficacy, and minimized risk for drug−drug interactions. Based on the available results and the favorable toxicological profile in rats, dogs, and cynomolgus monkeys, (*R*)-7 was selected as a clinical candidate for the treatment of coronary artery disease.

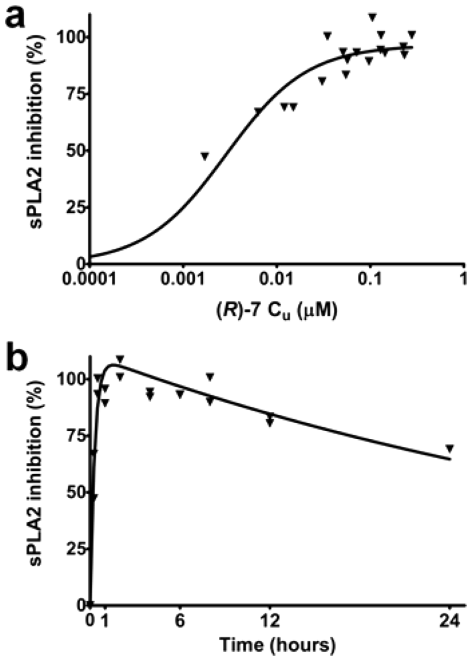

Figure 4. Vehicle-corrected plasma $sPLA_2$ activity inhibition: corresponding PK−PD relationship (a) and time course (b) following oral administration of 30 mg (*R*)-7 to cynomolgus monkeys (N = 2).

■ ASSOCIATED CONTENT

Supporting Information

The Supporting Information is available free of charge on the ACS Publications website at DOI: 10.1021/acsmedchemlett.6b00188.

Synthesis details for **2**−**9**, assay protocols, and X-ray data (PDF)

■ AUTHOR INFORMATION

Corresponding Authors

*(F.G.) Phone: +1-212-4780-822. E-mail: fabrizio.giordanetto@deshawresearch.com.

*(D.P.) Phone: +46 31 7065 663. E-mail: daniel.pettersen@astrazeneca.com.

Present Address

▽(F.G.) D. E. Shaw Research, 120 West 45th Street, New York, New York 10036, United States.

Author Contributions

The manuscript was written through contributions of all authors. All authors have given approval to the final version of the manuscript. Project leader, lead author F.G.; Author D.P.; Medicinal chemists D.P., P.N., M.D., I.S., L.K., N.S.; Bioscientists E.H.-C., B.R.; Enzyme assays U.K.; DMPK L.-O.L.; X-ray J.S., N.D., M.C.

Notes

The authors declare no competing financial interest.

Biographies

Fabrizio Giordanetto graduated in Medicinal Chemistry (Genoa, Italy) followed by his Ph.D. (London, UK) while working for the chemistry unit of Pharmacia−Pfizer (Italy). After positions at AstraZeneca (Sweden) as Principal Scientist and Project Leader and at Taros (Germany) as Head of Medicinal Chemistry, he has recently joined DE Shaw Research LLC (New York, USA) where he leads medicinal chemistry activities and drug discovery projects. During his career, he worked on several drug discovery programs resulting in multiple clinical candidates spanning oncology, CNS, inflammation, and cardiovascular indications and >100 peer-reviewed publications, book chapters, and international patents.

Daniel Pettersen received his Ph.D. in Organic Chemistry from the University of Gothenburg, Sweden, under the supervision of Prof. Per Ahlberg. Following graduation, he spent 2 years as a Post Doctoral Fellow at the University of Bologna, Italy, in the area of organocatalysis in the laboratories of Prof. Alfredo Ricci. In 2009 he was employed at Astrazeneca, Gothenburg, Sweden, working as a medicinal chemist in the cardiovascular and metabolic areas. Since 2012 he holds a Team Leader position in the Medicinal Chemistry department working on projects in various drug discovery phases. Recent publications include fibrinolysis inhibitors and sPLA2 inhibitors.

DOI: 10.1021/acsmedchemlett.6b00188
ACS Med. Chem. Lett. 2016, 7, 884−889

■ ACKNOWLEDGMENTS

Tomas Åkerud, Cristian Bodin, Kenth Hallberg, Thomas Olsson, and Hans-Georg Beisel are acknowledged for early lead generation work and useful discussions. Åsa Månson and Fana Hunegnaw are acknowledged for synthetic chemistry contributions.

■ REFERENCES

(1) Murakami, M.; Sato, H.; Miki, Y.; Yamamoto, K.; Taketomi, Y. A new era of secreted phospholipase A_2. *J. Lipid Res.* **2015**, *56*, 1248−1261.

(2) Singer, A. G.; Ghomashchi, F.; Le Calvez, C.; Bollinger, J.; Bezzine, S.; Rouault, M.; Sadilek, M.; Nguyen, E.; Lazdunski, M.; Lambeau, G.; Gelb, M. H. Interfacial kinetic and binding properties of the complete set of human and mouse groups I, II, V, X, and XII secreted phospholipases A_2. *J. Biol. Chem.* **2002**, *277*, 48535−48549.

(3) Kudo, I.; Murakami, M. Phospholipase A_2 enzymes. In *Prostaglandins and Other Lipid Mediators*; Elsevier, 2002; Vol. *68−69*, pp 3−58.

(4) Murakami, M.; Taketomi, Y.; Miki, Y.; Sato, H.; Hirabayashi, T.; Yamamoto, K. Recent progress in phospholipase A_2 research. In Cells to animals to humans. *Prog. Lipid Res.* **2011**, *50*, 152−192.

(5) Kimura-Matsumoto, M.; Ishikawa, Y.; Komiyama, K.; Tsuruta, T.; Murakami, M.; Masuda, S.; Akasaka, Y.; Ito, K.; Ishiguro, S.; Ito, K.; Ishiguro, S.; Morita, H.; Sato, S.; Morita, H.; Sato, S.; Ishii, T. Expression of secretory phospholipase A_2s in human atherosclerosis development. *Atherosclerosis* **2008**, *196*, 81−91.

(6) Hurt-Camejo, E.; Camejo, G.; Peilot, H.; Öörni, K.; Kovanen, P. Phospholipase A_2 in Vascular Disease. *Circ. Res.* **2001**, *89*, 298−304.

(7) Rosenson, R. S.; Hurt-Camejo, E. Phospholipase A_2 enzymes and the risk of therosclerosis. *Eur. Heart J.* **2012**, *33*, 2899−2909.

(8) Mallat, Z.; Lambeau, G.; Tedgui, A. Lipoprotein-Associated and Secreted Phospholipases A_2 in Cardiovascular Disease. *Circulation* **2010**, *122*, 2183−2200.

(9) Rosenson, R. S.; Gelb, M. H. Secretory phospholipase A_2: a multifaceted family of proatherogenic enzymes. *Curr. Cardiol Rev.* **2009**, *11*, 445−51.

(10) Shridas, P.; Webb, N. R. Diverse Functions of Secretory Phospholipases A_2. *Advances in Vascular Medicine* **2014**, *2014*, 1−11.

(11) Lind, L.; Simon, T.; Johansson, L.; Kotti, S.; Hansen, T.; Machecourt, J.; Ninio, E.; Tedgui, A.; Danchin, N.; Ahlström, H.; Mallat, Z. Circulating levels of secretory- and lipoprotein-associated phospholipase A_2 activities: relation to atherosclerotic plaques and future all-cause mortality. *Eur. Heart J.* **2012**, *33*, 2946−2954.

(12) For recent literature and references: Vasilakaki, S.; Barbayianni, E.; Leonis, G.; Papadopoulos, M. G.; Mavromoustakos, T.; Gelb, M. C.; Kokotos, G. Development of a potent 2-oxoamide inhibitor of secreted phospholipase A2 guided by molecular docking calculations. *Bioorg. Med. Chem.* **2016**, *24*, 1683−1695.

(13) Bradley, J. D.; Dmitrienko, A. A.; Kivitz, A. J.; Gluck, O. S.; Weaver, A. L.; Wiesenhutter, C.; Myers, S. L.; Sides, G. D. A randomized, double-blinded, placebo-controlled clinical trial of LY333013, a selective inhibitor of group II secretory phospholipase A_2, in the treatment of rheumatoid arthritis. *J. Rheumatol.* **2005**, *32*, 417−23.

(14) Nicholls, S. J.; Kastelein, J. J.; Schwartz, G. G.; Bash, D.; Rosenson, R. S.; Cavender, M. A.; Brennan, D. M.; Koenig, W.; Jukema, J. W.; Nambi, V.; Wright, R. S.; Menon, V.; Lincoff, A. M.; Nissen, S. E. Varespladib and cardiovascular events in patients with an acute coronary syndrome: the VISTA-16 randomized clinical trial. *JAMA* **2014**, *3*, 252−262.

(15) Ishimoto, Y.; Yamada, K.; Yamamoto, S.; Ono, T.; Notoya, M.; Hanasaki, K. Group V and X Secretory Phospholipase $A(_2)$s-Induced Modification of High-Density Lipoprotein Linked to the Reduction of Its Antiatherogenic Functions. *Biochim. Biophys. Acta, Mol. Cell Res.* **2003**, *1642*, 129−138.

(16) Hanasaki, K.; Yamada, K.; Yamamoto, S.; Ishimoto, Y.; Saiga, A.; Ono, T.; Ikeda, M.; Notoya, M.; Kamitani, S.; Arita, H. Potent Modification of Low Density Lipoprotein by Group X Secretory Phospholipase A_2 Is Linked to Macrophage Foam Cell Formation. *J. Biol. Chem.* **2002**, *277*, 29116−29124.

(17) de Beer, F. C.; Connell, P. M.; Yu, J.; de Beer, M. C.; Webb, N. R.; van der Westhuyzen, D. R. HDL Modification by Secretory Phospholipase A_2 Promotes Scavenger Receptor Class B Type I Interaction and Accelerates HDL Catabolism. *J. Lipid Res.* **2000**, *41*, 1849−1857.

(18) Erlanson, D. A. Introduction to fragment-based drug discovery. *Top. Curr. Chem.* **2011**, *317*, 1−32.

(19) Schevitz, R. W.; Bach, N. J.; Carlson, D. G.; Chirgadze, N. Y.; Clawson, D. K.; Dillard, R. D.; Draheim, S. E.; Hartley, L. W.; Jones, N. D.; Mihelich, E. D.; Olkowski, J. L.; Snyder, D. W.; Sommers, C.; Wery, J.-P. Structure-based design of the first potent and selective inhibitor of human non-pancreatic secretory phospholipase A_2. *Nat. Struct. Biol.* **1995**, *2*, 458−465.

(20) Lambeau, G.; Gelb, M. H. Biochemistry and physiology of mammalian secreted phospholipase A_2. *Annu. Rev. Biochem.* **2008**, *77*, 495−520.

(21) Pernas, P.; Masliah, J.; Olivier, J. − L.; Salvat, C.; Rybkine, T.; Bereziat, G. Type II Phospholipase A_2 recombinant overexpression enhance stimulated arachidonic acid release. *Biochem. Biophys. Res. Commun.* **1991**, *178*, 1298−1305.

(22) Kristensen, J.; Lysén, M.; Vedsö, P.; Begtrup, M. Synthesis of ortho substituted arylboronic esters by in situ trapping of unstable lithio intermediates. *Org. Lett.* **2001**, *10*, 1435−1437.

(23) Hsiang, B.; Zhu, Y.; Wang, Z.; Wu, Y.; Sasseville, V.; Yang, W. P.; Kirchgessner, T. G. A novel human hepatic organic anion transporting polypeptide (OATP2). Identification of a liver-specific human organic anion transporting polypeptide and identification of rat and human hydroxymethylglutaryl-CoA reductase inhibitor transporters. *J. Biol. Chem.* **1999**, *274*, 37161−37168.

(24) Mizuno, N.; Niwa, T.; Yotsumoto, Y.; Sugiyama, Y. Impact of drug transporter studies on drug discovery and drug development. *Pharmacol Rev.* **2003**, *55*, 425−461.

(25) Shitara, Y.; Horie, T.; Sugiyama, Y. Transporters as a determinant of drug clearance and tissue distribution. *Eur. J. Pharm. Sci.* **2006**, *27*, 425−446.

(26) Hurt-Camejo, E.; Andersen, S.; Standal, R.; Rosengren, B.; Sartipy, P.; Stadberg, E.; Johansen, B. Localization of Non Pancreatic Secretory Phospholipase A_2 in Normal and Atherosclerotic Arteries: Activity of the Isolated Enzyme on Low Density Lipoproteins. *Arterioscler., Thromb., Vasc. Biol.* **1997**, *17*, 300−309.

DOI: 10.1021/acsmedchemlett.6b00188
ACS Med. Chem. Lett. 2016, 7, 884−889